

## Nonequilibrium Periodic Structures Induced by Rotating and Static Fields in a Lyotropic Nematic Liquid Crystal

Michael R. Kuzma

*Physics Department, Temple University, Philadelphia, Pennsylvania 19122*

(Received 21 February 1986)

Nonequilibrium periodic textures are induced by a magnetic field  $H$  applied to the aligned uniaxial (negative diamagnetic anisotropy) lyotropic nematic phase of the potassium laurate-decanol-water system. Two cases are studied: a rotating field and a static field. For the rotating field a transient one-dimensional structure results. With the static field, the appearance and decay of a two-dimensional lattice structure is observed. In both cases the dependence of the lattice periodicity on  $H$  is measured and compared to recent theories.

PACS numbers: 61.30.Gd, 47.20.-k, 61.30.Eb

A body of recent work has been devoted to the study of hydrodynamic periodic textures in liquid crystals induced by magnetic reorientation of the optic axis  $\mathbf{n}$ .<sup>1-4</sup> A first theoretical study of the occurrence of the textures was carried out by Guyon, Meyer, and Salan (GMS)<sup>5</sup> who were stimulated by the observations of Carr.<sup>6</sup>

The patterns are generated by application of a destabilizing magnetic field to an initially uniformly aligned sample. As the director field reorients to minimize the magnetic energy, the coupling between elastic response and flow fields may allow a spatially periodic reorientation mode  $\delta\mathbf{n}(q_c, s_c)$ , of wave number  $q_c$  and growth rate  $s(q_c)$ , to increase faster than a homogeneous mode  $s(q=0)$ . The patterns studied in this work are transient, decaying on time scales characteristic of the viscosities of the liquid crystal. When a typical sample is observed between crossed polarizers in transmitted light, the periodicity of the director field generally appears as a series of parallel stripes. The wavelength of the structure varies with applied field and sample size, and this dependence is used to qualitatively identify a working theoretical model.

Recent work of the Brandeis group has primarily concentrated on the one-dimensional reorientation patterns in nematic suspensions of tobacco mosaic virus<sup>2</sup> and racemic polybenzylglutamate mixtures.<sup>1</sup> Periodic textures have also been studied in the lyotropic nematic phase of disodium chromoglycate-water.<sup>3</sup>

In this Letter, we investigate periodic textures obtained in a lyotropic nematic phase of negative diamagnetic anisotropy ( $\chi_a < 0$ ): the  $N_L$  phase of potassium laurate (KL), 1-decanol, and  $D_2O$ . The simplest model of this phase has the surfactant arranged in discoidal micelles which through anisotropic steric and van der Waals interactions align on the average to form a uniaxial nematic.

Samples of the  $N_L$  phase are placed in a rotating or static magnetic field  $H$ . The rotating samples form a one-dimensional structure which is described by the GMS theory.<sup>5</sup> With the static field aligned parallel to

the initial director, the reorientation displays a remarkable transient one-dimensional (square lattice) periodicity. We believe that this is the first observation of spontaneous two-dimensional reorientation patterns in nematics.

The KL was prepared in the standard way.<sup>7</sup> Samples of KL, 1-decanol, and  $D_2O$  were mixed by magnetic stirring in airtight culture tubes (Kimax) and allowed to sit for at least 1-2 weeks before use. Capillary action was used to draw samples into rectangular capillaries (Vitro Dynamics, New Jersey) of various sizes, which were then carefully sealed with a torch. For this work the sample composition was KL/1-decanol/ $D_2O$  = 26.36/6.24/67.40 wt. %—this gave an  $N_L$  phase at room temperature (19°C).

Samples of the  $N_L$  phase spontaneously align to a uniaxial homeotropic texture (the director—optic axis—aligns perpendicularly to the walls of a rectangular glass capillary). Uniform alignment proceeds entirely by surface interaction. Apparently the polar groups of the KL enforce a uniformly oriented first layer next to the glass, and this supplies a surface field strong enough to realign disturbed textures in even relatively thick samples ( $\sim 1$  mm). A magnetic field applied parallel to  $\mathbf{n}$  causes realignment provided  $H > H_c$ , where the threshold field  $H_c = (K_{33}/\chi_a)^{1/2} \times (\pi/d)$ ;  $K_{33}$  is the bend elastic constant and  $d$  is the sample thickness. This situation is interesting in that it possesses a degeneracy in tilt-angle directions perpendicular to the optic axis.

For the first case we select a geometry which removes the degeneracy by rotating the magnetic field in the  $y$ - $z$  plane, placing the long capillary axis parallel to  $x$ . For simplicity we have chosen a reference frame in which the director remains fixed and  $\mathbf{H}(t) = H_0 \times (0, \sin\alpha, \cos\alpha)$ ,  $\alpha = \omega t$ . The rotation speeds,  $\nu = \omega/2\pi$ , were kept below the values for which centrifugal forces caused significant flow ( $\approx 300$  rpm for  $L = 4$  mm and  $d = 0.2$  mm sample width and thickness, respectively). A lower limit to the rotation speed for a given  $H$  is set by<sup>8</sup>  $\nu_c = \chi_a H^2 / 4\pi\gamma_1 \approx 1$  rpm ( $\chi_a = 10^{-8}$

cgS,  $\gamma_1 = 10 \text{ P}$ ,<sup>9</sup>  $H \sim 10^4 \text{ G}$ ); for  $\nu$  significantly above  $\nu_c$  the director cannot follow the field and a time average may be performed. It is easy to show that in this limit  $H_{cr} = 2^{1/2} H_{cs}$  where the subscripts imply the critical fields for the Fréedericksz transition in the rotating and static cases, respectively. We set  $\nu = 120 \text{ rpm}$  for this study. Trials at 90 and 250 rpm did not change the basic results.

At sufficiently high rotation speeds, for the geometry mentioned above (translation invariance in the  $y$  direction), the linearized nematodynamic equations for the velocity field  $\mathbf{v} = (v_x, 0, v_z)$  and director  $\mathbf{n} = (n_x, 0, 1)$  take the form

$$\begin{aligned} \rho \dot{v}_x = & -\partial_x p + \nu_1 \partial_z \dot{n}_x + \nu_2 \partial_{xx} v_x \\ & + \nu_3 \partial_{zz} v_x + \nu_4 \partial_{zx} v_z, \end{aligned} \quad (1a)$$

$$\begin{aligned} \rho \dot{v}_z = & -\partial_z p + \nu_5 \partial_x \dot{n}_x + \nu_6 \partial_{xz} v_x \\ & + \nu_7 \partial_{xz} v_z + \nu_8 \partial_{zz} v_z, \end{aligned} \quad (1b)$$

$$\begin{aligned} \gamma_1 \dot{n}_x = & -\alpha_z \partial_z v_x - \alpha_3 \partial_x v_z + K_{11} \partial_{xx} n_x \\ & + K_{33} \partial_{zz} n_x + \frac{1}{2} |\chi_a| H^2 n_x. \end{aligned} \quad (1c)$$

We further assume incompressibility,  $\nabla \cdot \mathbf{v} = 0$ . Here  $\rho$  is the mass density, the  $\nu_i$  are each a certain combination of Leslie coefficients  $\alpha_i$ ,  $\gamma_1$  is a rotational viscosity,  $K_{11}$  and  $K_{33}$  are elastic constants for splay and bend, respectively, and  $\partial_{ij} = \partial^2 / \partial x_i \partial x_j$ ,  $\dot{n} = \partial n / \partial t$ . The factor of  $\frac{1}{2}$  in front of  $\chi_a$  arises from the time average of the rotating field; for the static field this factor is absent.

Equations (1) are derived for a homeotropic geometry; however, they are identical in form to the Navier-Stokes and torque equations derived by GMS for a planar geometry. The only difference is that the  $\nu_i$  are a different combination of the  $\alpha_i$ .

We assume the boundary conditions  $v_z = n_x = \partial_z v_x = 0$  at  $z = 0$  and  $d$  (free boundaries). Exact solutions for rigid boundaries<sup>1</sup> indicate that, except for a layer of large shear close to the surfaces, the free solutions provide an adequate description of the growth modes through the bulk of the system.

Following GMS the solutions to Eq. (1) can be written as

$$v_x = v_0 k \exp(st) \sin qx \cos kz, \quad (2a)$$

$$v_z = -v_0 q \exp(st) \cos qx \sin kz, \quad (2b)$$

$$n_x = n_0 \exp(st) \sin qx \sin kz. \quad (2c)$$

For free boundaries, the wave number  $k = \pi/d$ . The wave number  $q = 2\pi/\lambda$ , where  $\lambda$  is the wavelength of the periodic structure. Substituting Eq. (2) into Eq. (1) we arrive at an expression for the growth rate  $s = s(q, k, H)$ , which again is identical in form to that obtained in GMS. For sufficiently large  $h = H/H_c$ ,  $s$

has a maximum for a finite wave number ( $q_c = 2\pi/\lambda_c$ ) determined from  $\partial\omega/\partial q = 0$ . We do not know explicit values for the material parameters but for  $h > 2.4$  a numerical solution for  $\lambda$  can be placed in the form

$$(d/\lambda_c)^2 = a_0 H + a_1, \quad (3)$$

which permits a simple qualitative comparison with experiment. The coefficients  $a_0$ ,  $a_1$  depend upon material parameters but are constant at a given temperature.

Figure 1 demonstrates a typical periodic texture obtained in a rotating field. The wavelength  $\lambda_{cr}$  of the transient periodic texture is presented as function of  $H$  in Fig. 2. The limit established on the critical field is  $2 \text{ kG} < H_{cr} < 2.5 \text{ kG}$ . Since we could not determine  $H_{cr}$  accurately, it was absorbed into the constant  $a_0$  in Eq. (1). To within experimental error we find qualitative agreement with the theory of GMS.

The second case which considers static fields was somewhat more surprising in its behavior under reorientation. With  $H (> H_{cs})$  oriented parallel to the director of an initially uniform homeotropic alignment we noticed the appearance of large ( $\approx 500 \mu\text{m}$ ) regions with a remarkable two-dimensional periodicity [Fig. 3(a)]. The lattice texture is transient, decaying in a few hours for  $H = 10 \text{ kG}$ .

One- and two-dimensional patterns have been observed in smectics and cholesterics; however, these systems have broken translational symmetry allowing an undulation instability,<sup>10</sup> which is in principle a static deformation.

Upon rotation of the microscope stage one can easily see that the lattice is composed of an array of  $\pm 1$



FIG. 1. Photomicrograph of periodic texture in a rotating sample of the  $N_L$  phase of potassium laurate-decanol- $D_2O$ . The rotation axis is perpendicular to the stripes. The polarizer and analyzer are parallel to the short and long edges of the picture, respectively. The sample thickness  $d = 0.1 \text{ mm}$ ,  $T = 19^\circ\text{C}$ , and the average spacing of the stripes  $\lambda_{cr} = 50 \mu\text{m}$ .  $H = 10 \text{ kG}$ .

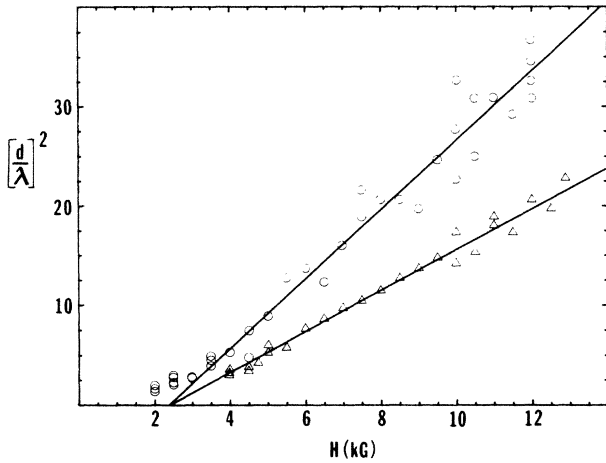
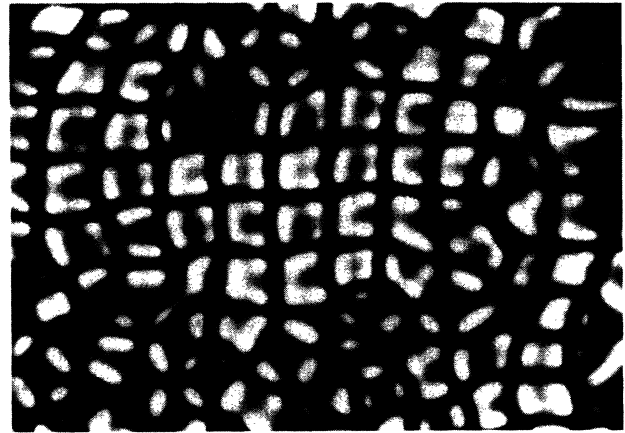


FIG. 2. Inverse square of periodic structure vs magnetic field. Circles and triangles denote the static and rotating cases, respectively. Sample thickness  $d = 200 \mu\text{m}$ . For Eq. (3)  $a_0 = 3.5$ ,  $a_1 = -8.3$  for circles;  $a_0 = 2.1$ ,  $a_1 = -4.9$  for triangles.

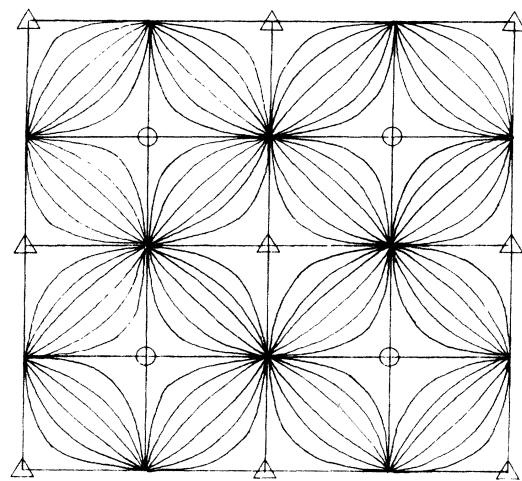
singularities. The mathematical structure of the director field of isolated singularities in this case is well known and was discussed some time ago by Rapini.<sup>11</sup> Following Ref. 11 we use the term magnetic umbilics to describe the singularities. Umbilics are distinguished from true singularities in that their core is spread out over a characteristic length  $\xi = (\delta d/\pi) \times ([H/H_c]^2 - 1)^{-1/2}$ , where  $\delta$  is a certain ratio of Frank elastic constants.

The observed texture varies through the thickness of the cell. When the focal plane is near the top of the cell the brushes form a square lattice of wavelength  $2\lambda_{cr}$ . As one moves to the center of the sample Fig. 3 results. Near the bottom of the cell a transposed lattice again of wavelength  $2\lambda_{cs}$  appears with brushes centered on sites which are dual to the top lattice. A sketch of a structure composed of splay-bend umbilics of strength  $s = \pm 1$  is given in Fig. 3(b). If one starts in the center of the sample with the crossed polars oriented along the fundamental lattice directions (wavelength  $\lambda_{cs}$ ) and then rotates both polars or the stage through  $\pi/4$ , a lattice of brushes appears with a wavelength  $\lambda_{cs}/2^{1/2}$ . It is easily verified that the texture of Fig. 3(b) reproduces this property (excluding of course nonlinearities present in the real system which affect the intensities of the brushes). Although the texture of Fig. 3(b) is not unique, we found that it can be extended into three dimensions in a simple way consistent with the above observations, unlike other possible textures envisioned. An *a priori* determination of the texture might require a minimization of the elastic energy similar to the numerical minimization employed for textures of the blue phase.<sup>12</sup>

The behavior of the lattice constant  $\lambda_{cs}$  versus mag-



(a)



(b)

FIG. 3. (a) Photomicrograph of square lattice reorientation pattern in the KL system. Focal plane is in center of sample. Polars, same orientation as Fig. 1. Sample thickness  $0.2 \text{ mm}$ , average periodicity  $\lambda_{cs} = 38 \mu\text{m}$ .  $H = 10 \text{ kG}$ . (b) Sketch of texture proposed for (a). Triangles and circles are located in centers of  $S = -1$  bend umbilics; adjacent are  $S = +1$  splay umbilics. The circles indicate vertices of brushes of square lattice of periodicity  $2\lambda_{cs}$  for focal plane in (say) top half of sample, the triangles for bottom half. The straight lines of (b) correspond to the brushes of (a) with the polars oriented as in Fig. 1.

netic field  $H$  is reproduced in Fig. 2. In this case the limits on the critical field were  $1 \text{ kG} < H_{cs} < 1.5 \text{ kG}$ . We note a qualitative accord with the theoretical relation  $H_{cr}/H_{cs} = 1^{1/2}$ .<sup>8</sup> Again among other forms available, the data followed Eq. (1) with new values of  $a_0$  and  $a_1$ . The unavoidable presence of dislocations in the square lattice resulted in relatively noisier data for this case compared to  $\lambda_{cr}$ , but the similarity of the data for both the rotating and static cases indicates a probable similarity in the underlying physical phenomenon.

Although the preference of the square lattice over, say, a triangular lattice is easily explained by topological considerations, the appearance of the lattice indicates the importance of including nonlinear terms in the analysis [barring the possible accidental equality of two growth rates,  $S_\alpha$  ( $\alpha=1,2$ ), of perpendicular polarization]. Further theoretical studies are needed.

The above features are complicated by the fact that the texture is transient, decaying within hours ( $H=10$  kG,  $d=0.2$  mm) through annihilation of  $+1$ ,  $-1$  umbilics to an unaligned planar texture with isolated  $\pm 1$  umbilics. The results of Fig. 2 represent direct measurements of the lattice constants  $\lambda_{cs}$  and  $\lambda_{cr}$  at the earliest time they become observable and reproducible.

The square lattice of Fig. 3 results from the degeneracy of tilt directions for the optic axis. Simply tilting the sample cell removes this degeneracy and a rectangular lattice is formed with the direction of the largest spacing in the tilt plane defined by  $H$  and the sample normal. For large enough tilt ( $45^\circ$ ), weak stripes appear parallel to the tilt plane.

A second mechanism to break the tilt degeneracy is to use aligned biaxial samples. This possibility is being explored.

The author would like to thank the Pew Memorial Foundation for an equipment grant. The help of D. Rose in plotting Fig. 2 is appreciated. I would also

like to thank D. Forster for an illuminating discussion.

<sup>1</sup>A. J. Hurd, S. Fraden, F. Lonberg, and R. B. Meyer, *J. Phys. (Paris)* **46**, 905 (1985).

<sup>2</sup>S. Fraden, A. J. Hurd, R. B. Meyer, M. Cahoon, and D. L. D. Caspar, *J. Phys. (Paris), Colloq.* **46**, C3-85 (1985).

<sup>3</sup>Y. W. Hui, M. R. Kuzma, M. San Miguel, and M. M. Labes, *J. Chem. Phys.* **83**, 288 (1985); D. Rose, J. Swift, and M. R. Kuzma, unpublished.

<sup>4</sup>J. Charvolin and Y. Hendrix, *J. Phys. (Paris), Lett.* **41**, L597 (1980).

<sup>5</sup>E. Guyon, R. Meyer, and J. Salan, *Mol. Cryst. Liq. Cryst.* **54**, 261 (1979).

<sup>6</sup>E. F. Carr, *Mol. Cryst. Liq. Cryst.* **34**, 159 (1977).

<sup>7</sup>P. Boonbrahm and A. Saupe, *Mol. Cryst. Liq. Cryst.* **109**, 225 (1984).

<sup>8</sup>F. Brochard, L. Leger, and R. B. Meyer, *J. Phys. (Paris), Colloq.* **36**, C1-209 (1975).

<sup>9</sup>This estimate is obtained from the similar  $N_L$  system, decylammonium chloride-ammonium chloride-water; see T. Haven, D. Armitage, and A. Saupe, *J. Chem. Phys.* **75**, 352 (1981).

<sup>10</sup>P. G. de Gennes, *The Physics of Liquid Crystals* (Clarendon, Oxford, 1975); J. M. Delrieu, *J. Chem. Phys.* **60**, 1081 (1974).

<sup>11</sup>A. Rapini, *J. Phys. (Paris)* **34**, 629 (1973); A. Rapini, L. Leger, and A. Martinet, *J. Phys. (Paris), Colloq.* **36**, C1-189 (1975).

<sup>12</sup>M. J. Sammon, *Mol. Cryst. Liq. Cryst.* **89**, 305 (1982).

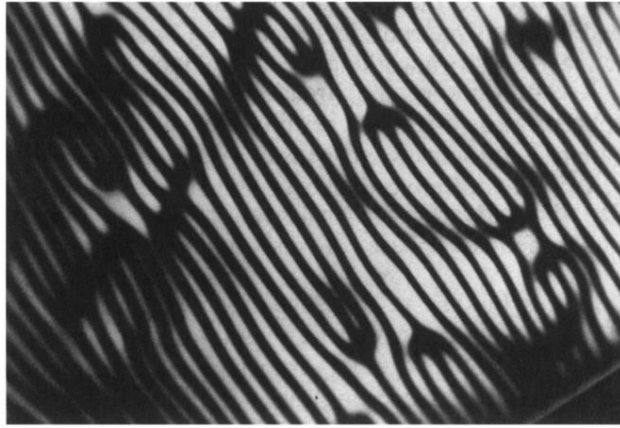
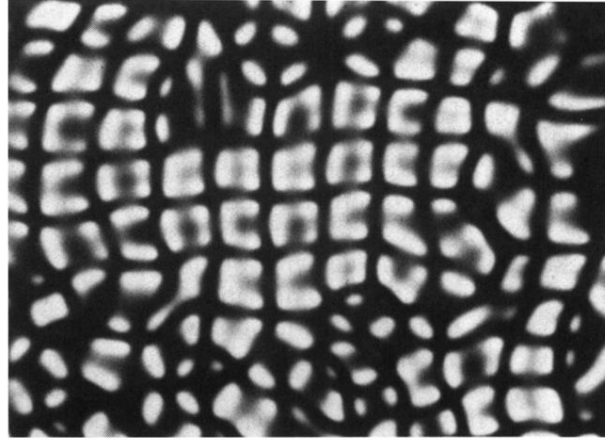
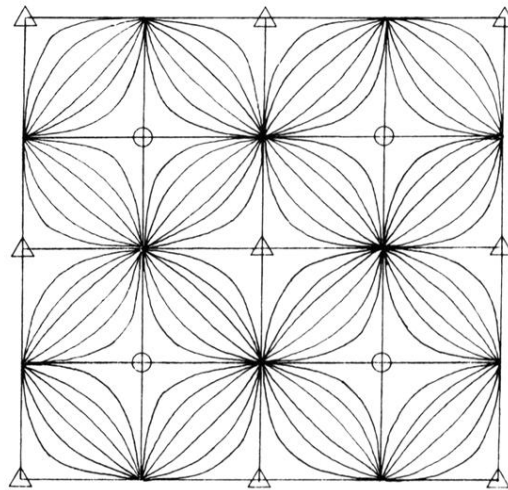


FIG. 1. Photomicrograph of periodic texture in a rotating sample of the  $N_L$  phase of potassium laurate-decanol- $D_2O$ . The rotation axis is perpendicular to the stripes. The polarizer and analyzer are parallel to the short and long edges of the picture, respectively. The sample thickness  $d = 0.1$  mm,  $T = 19^\circ C$ , and the average spacing of the stripes  $\lambda_{cr} = 50$   $\mu m$ .  $H = 10$  kG.



(a)



(b)

FIG. 3. (a) Photomicrograph of square lattice reorientation pattern in the KL system. Focal plane is in center of sample. Polars, same orientation as Fig. 1. Sample thickness 0.2 mm, average periodicity  $\lambda_{cs} = 38 \mu\text{m}$ .  $H = 10 \text{ kG}$ . (b) Sketch of texture proposed for (a). Triangles and circles are located in centers of  $S = -1$  bend umbilics; adjacent are  $S = +1$  splay umbilics. The circles indicate vertices of brushes of square lattice of periodicity  $2\lambda_{cs}$  for focal plane in (say) top half of sample, the triangles for bottom half. The straight lines of (b) correspond to the brushes of (a) with the polars oriented as in Fig. 1.